Cooperativity in the binding of avidin to biotin-lipid-doped Langmuir-Blodgett films

ARTICLE *in* LANGMUIR · NOVEMBER 1993

Impact Factor: 4.46 · DOI: 10.1021/la00035a069

3 AUTHORS, INCLUDING:

Wiliiam M Reichert
Duke University
60 PUBLICATIONS **3,082** CITATIONS

SEE PROFILE

Cooperativity in the Binding of Avidin to Biotin-Lipid-Doped Langmuir-Blodgett Films

Shulei Zhao,† D. S. Walker, and W. M. Reichert*

Department of Biomedical Engineering and the Center for Emerging Cardiovascular Technologies, Duke University, Durham, North Carolina 27708-0281

Received April 13, 1993. In Final Form: July 22, 1993®

Monolayers of arachidic acid (AA) doped with either biotinylated DPPE (B-DPPE) or a chain extended biotinylated DPPE (B-x-DPPE) were deposited onto alkylsilane treated surfaces of quartz evanescent fiber optic sensors (EFO) by the Langmuir-Blodgett (LB) technique. The surface-modified EFOs were used to obtain binding isotherms of fluorescein-labeled avidin to the biotin-lipid-doped LB films. Hyperbolic binding isotherms were observed for all B-DPPE doped LB films and for B-x-DPPE doped films with <0.63 mol % biotin lipid. Sigmoid or positively cooperative binding isotherms were observed for all LB films with ≥0.63 mol % B-x-DPPE. A mathematical expression for protein binding to a two-dimensional array of receptors that takes protein-protein interaction into account was used to quantitatively assess the cooperativity observed in the isotherms. Attenuated total reflection Fourier transform infrared (ATR-FTIR) spectroscopy was used to address speculation that cooperativity resulted from a conformational change in avidin. ATR-FTIR results show that avidin experienced significant conformational changes when bound to biotin lipids in the LB films, wheras no conformational change was observed for avidin nonspecifically bound to biotin-free LB films.

Introduction

Supported lipid monolayers or bilayers have been widely used as model membranes for studying protein-membrane interactions.[1-4] The majority of these reports studied antibody binding to supported phospholipid layers containing hapten groups at the solid-liquid interface. Alternatively, Ahlers et al. studied the binding of the protein avidin to monolayers containing biotin groups as an analog of the biomembrane system.[5] The avidin-biotin system is an attractive model for protein-receptor binding because of its high binding affinity, high degree of characterization, and broad technological applications.[6]

Recently, we used the avidin-biotin lipid model to investigate the influence of receptor density and receptor accessibility on the kinetics of targeted protein binding to solid surfaces.[7,8] Although primarily employed for chemical sensing,[9] the evanescent fiber optic (EFO) system provides a convenient, efficient, and inexpensive method of monitoring protein binding at the solid-liquid interface. In the current paper we use the EFO system to obtain isotherms of avidin binding to biotin-lipid-doped Langmuir-Blodgett (LB) monolayers of arachidic acid (AA) at the solid-solution interface. AA provides a stable and reasonably inert matrix that is readily doped from 0 to 100 mol % with one of two biotinylated phospholipids: biotinylated DPPE (B-DPPE) and a chain extended biotinylated DPPE (B-x-DPPE), with the latter presenting a more accessible biotin group at the surface of the LB film.[8] The different accessibilities of the biotin group of B-DPPE and B-x-DPPE in the LB film are illustrated schematically in Figure 1.

All of the avidin binding isotherms reported in this paper were hyperbolic in shape, except for surfaces with ≥0.63 mol % B-x-DPPE that produced sigmoid binding isotherms. Interestingly, 0.63 mol % is close to the minimum receptor density required to bind a monolayer of avidin.[8] These results suggest that avidin binding to biotin lipids in the LB film was essentially noncooperative, except when there was a sufficiently high density of the more accessible B-x-DPPE where positively cooperative binding was observed. A model for the isotherm of protein binding to a two-dimensional array of receptors was developed and used to analyze the experimental data. Cooperativity stemming from protein-protein interaction is taken into account in this model.

Speculation that the observed cooperativity resulted from a conformational change in avidin led to collecting the infrared spectra of surface-bound avidin in a Fourier transform infrared (FTIR) spectrometer equipped with a liquid flow cell and attenuated total reflection (ATR) optics. The amide I, II, and III bands of avidin are readily observed by ATR-FTIR,[10] and shifts in the ratio of the amide II to amide I band intensities are a common indicator of protein conformational change.[11] All infrared spectra presented in this paper originated from monolayer and submonolayer avidin films that were background subtracted of contributions from the ATR crystal, the LB film, and the bulk solution. From the ratio of the amide II to amide I intensities, it appears that avidin bound to biotin lipids in the LB films experienced significant loss of native conformation, whereas no evidence of a confor-

* To whom correspondence should be addressed.
† Present address: Department of Ophthalmology and Visual Science, Yale University School of Medicine, New Haven, CT 06510.
® Abstract published in *Advance ACS Abstracts*, October 1, 1993.

(1) Hafeman, D. G.; von Tscharner, V.; McConnell, H. M. *Proc. Natl. Acad. Sci. U.S.A.* **1981**, *78*, 4552-4556.
(2) Tamm, L. K.; McConnell, H. M. *Biophys. J.* **1985**, *47*, 105-113.
(3) Kalb, E.; Engel, J.; Tamm, L. K. *Biochemistry* **1990**, *29*, 1607-1613.
(4) Pisarchick, M. L.; Thompson, N. L. *Biophys. J.* **1990**, *58*, 1253-1249.
(5) Ahlers, M.; Müller, W.; Reichert, A.; Ringsdorf, H.; Venzmer, J. *Angew. Chem., Int. Ed. Engl.* **1990**, *29*, 1269-1285.
(6) Wilchek, M.; Bayer, E. A., Eds. *Methods in Enzymology*; Academic: San Diego, CA, 1990; No. 184.
(7) Zhao, S.; Reichert, W. M. *ACS Symp. Ser.* **1992**, *No. 493*, 123-134.
(8) Zhao, S.; Reichert, W. M. *Langmuir* **1992**, *8*, 2785-2791.
(9) Thompson, R. B.; Ligler, F. S. In *Biosensors with Fiberoptics*; Wise, D. L., Wingard, L. B., Eds.; The Humana Press: Totowa, NJ, 1991; pp 111-137.
(10) Barbucci, R.; Magnani, A.; Roncolini, C.; Silvestri, S. *Biopolymers* **1991**, *31*, 827-834.
(11) Kato, K.; Matsui, T.; Tanaka, S. *Appl. Spectrosc.* **1987**, *41*, 861-865.

0743-7463/93/2409-3166$04.00/0

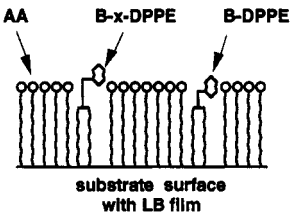

Figure 1. Arachidic acid (AA) monolayers deposited on the fiber-optic sensor or ATR crystal surface. The monolayer contains one of two biotinylated phospholipids, either B-DPPE or B-x-DPPE.

mational change was observed for avidin nonspecifically bound to biotin-free LB films.

Theory

A Model for Cooperative Binding Isotherms. Consider protein binding to a receptor on a surface and perturbations in the binding energy caused by neighboring receptors. Let $\Delta G°$ be the standard free energy change accompanying the binding of the protein molecule to a receptor if all the neighboring receptors are all free of bound protein. If one of the neighboring receptors is bound by a protein molecule, the presence of this molecule may perturb the standard free energy change by δG_1, i.e. $\Delta G = \Delta G° + \delta G_1$. In general, if n neighbors of the receptor are bound with protein molecules, the free energy change is

$$\Delta G = \Delta G° + n\sum_{i=0}^{n} \delta G_i \tag{1}$$

where $\delta G0 = 0$ and δG_i ($i = 1, 2, ..., n$) is the free energy perturbation induced by a protein molecule bound to the ith neighboring receptor. Substituting eq 1 for ΔG in eq A5 (see Appendix A), we obtain an expression for the association constant K

$$K = K_0 \prod_{i=0}^{n} \eta_i \tag{2}$$

where

$$\eta_i = \exp(-\delta G_i/RT) \tag{3}$$

$$K_0 = K_\alpha \exp(-\Delta G°/RT) \tag{4}$$

and where η_i is the *cooperativity coefficient* that characterizes the level of protein–protein interaction between bound neighboring molecules and K_0 is the *intrinsic association constant* of the protein binding to its receptor without any interference from other neighboring bound protein molecules.[12] Assuming the perturbation of the free energy change induced by each neighbor is equivalent (i.e. $\delta G_i = \delta G$ or $\eta_i = \eta$ for $i = 1, ..., n$), eq 2 becomes

$$K = \eta^n K_0 \tag{5}$$

It is apparent from eq 3 and eq 5 that $\delta G < 0$, $\delta G = 0$, and $\delta G > 0$ correspond to positive cooperativity ($\eta > 1$ and $K > K_0$), noncooperativity ($\eta = 1$ and $K = K_0$), and negative cooperativity ($\eta < 1$ and $K < K_0$), respectively.

For the bimolecular reaction of protein A and its receptor B (see eq A1 in Appendix A), the total number of receptors (or the initial number of free receptors) is the sum of the numbers of free and bound receptors, i.e. $[B]_0 = [B] + [AB]$, where $[B]_0$ is the initial surface density of the receptor. By denoting $x_0 = [B]/[B]_0$ and $x_1 = [AB]/[B]_0$, and utilizing eq 5, a general expression for a protein binding isotherm can be derived from the definition of K (see eq A4 in Appendix A)

$$\eta^n K_0[A] = \frac{x_1}{1 - x_1} \tag{6}$$

where [A] is the bulk protein concentration and x_1 is the fraction of bound receptors. Equation 6 can also be written as

$$x_1 = \frac{\eta^n K_0[A]}{1 + \eta^n K_0[A]} \tag{7}$$

Setting $\eta = 1$ in eq 7 yields the Langmuir isotherm model which is clearly a special noncooperative case of the more general binding isotherm expression.

Protein Binding to a Two-Dimensional Receptor Array. To model protein binding to its receptors on a surface, it is necessary to assume that the receptors are regularly distributed. More discussion of various distribution geometries is available elsewhere.[13-15] For reasons discussed later, it is assumed in this paper that the protein receptors are distributed in a square lattice (see Appendix B1), where the number of nearest neighboring receptors to each individual receptor is four ($z = 4$). Intuitively, the number of bound neighbors of a given receptor (n in eq 6 or eq 7) increases with the fraction of bound receptors (x_1 in eq 6 or eq 7). However, the only appropriate value of n that can be used in eq 6 or eq 7 is the average value n for all receptors. The average value of n for the case of a square receptor distribution is derived in Appendix B, where the receptor array is assumed to be infinite.

The result of this derivation is simply $n = 4x_1$ (see eq B4 in Appendix B) where $x_1 = (AB)/[B]_0$. Letting $\omega = \eta^n$ for convenience, eq 6 becomes

$$\omega^{x_1} K_0[A] = \frac{x_1}{1 - x_1} \tag{8}$$

where for a square lattice of receptors $\omega = \eta^4$. Finally, assuming that fluorescence intensity (F) is linearly proportional to the amount of protein bound to the sensor surface, i.e. $F = x_1 F_{max}$, then eq 8 becomes

$$\omega^{(F/F_{max})} K_0[A] = \frac{F}{F_{max} - F} \tag{9}$$

where F_{max} is the fluorescence intensity measured when all the receptors are bound by the protein.

Materials and Methods

Preparation of the EFO Surface. Details regarding the fabrication and operation of the EFO, the LB deposition on the EFO sensing tip, and the fluorescence signal detection of surface bound protein are available elsewhere.[7,8] Briefly, arachidic acid (AA, Eastman Kodak, Rochester, NY) monolayers containing precise amounts of biotin lipids were deposited on the sensing tip of a quartz EFO by the Langmuir–Blodgett (LB) technique in a Teflon-lined film balance (NIMA, Coventry, UK). The EFO quartz surface was treated with dichlorodimethylsilane (DDS, Aldrich, Milwaukee, WI) to render it hydrophobic, resulting in the deposition of a head-group-out oriented LB monolayer film at the quartz surface upon the down stroke into the aqueous subphase (Figure 1). A flow cell arrangement was used to introduce fluorescently labeled avidin to the sensor surface. The relative amount of surface-bound avidin was determined by EFO

(12) Tanford, C. *Physical Chemistry of Macromolecules*; John Wiley & Sons, New York, 1961; pp 535.

(13) Stankowski, S. *Biochim. Biophys. Acta* **1983**, *735*, 341–351.
(14) Stankowski, S. *Biochim. Biophys. Acta* **1983**, *735*, 352–360.
(15) Stankowski, S. *Biochim. Biophys. Acta* **1984**, *777*, 167–182.

fluorescence spectroscopy. The LB films contained one of two biotinylated phospholipid receptors: *N*-(biotinoyl)dipalmitoyl-L-α-phosphatidylethanolamine (B-DPPE) or *N*-(6-(biotinoyl)-amino)hexanoyl)dipalmitoyl-L-α-phosphatidylethanolamine (B-x-DPPE) (Molecular Probes, Eugene, OR). B-x-DPPE is the same as B-DPPE, except that B-x-DPPE has an extra spacer between the phospholipid and the biotin group.[16] This extended the biotin group of B-x-DPPE further above the lipid monolayer than was the biotin group of B-DPPE (Figure 1). Stock solutions of AA and B-DPPE or B-x-DPPE in chloroform were carefully combined to produce spreading solutions with biotin lipid and arachidic acid in various molar ratios. These solutions were spread at the air–water interface, compressed to 35 mN/m, and deposited on the EFO surface as described elsewhere.[7,8] Note that each EFO surface tested contained AA and either B-DPPE or B-x-DPPE, but not both biotin lipids as suggested in Figure 1. The transfer ratio of the LB deposition was high (~0.90).[17] Therefore, the density of biotin lipids on the EFO surface was taken to be equal to the surface density at the air–water interface before the transfer.

Avidin Binding Isotherms. Fluorescein isothiocyanate (FITC) labeled avidin (Sigma, St. Louis, MO) was dissolved to concentrations ranging from 0.05 to 10 μg/mL in 0.01 M phosphate buffered saline (PBS, pH 7.5) with 0.5 M NaCl. Preparation of the sensor and its assemblage into the flow cell followed the same procedure described previously.[7] First, the most dilute avidin solution was introduced into the flow cell and remained for 30 min. The fluorescence emission from avidin bound to the sensor surface was measured before and after the protein solution was gently flushed out of the flow cell with PBS. The fluorescence intensities measured before and after PBS rinse were essentially the same, suggesting that only surface-bound protein contributed to fluorescence collected by the sensor system. This procedure was repeated for 8 to 12 solutions of increasing avidin concentration. Each experiment ended with collecting a reference spectrum from 0.4 mg/mL fluorescein solution which was used for data normalization.[7,17] A high FITC concentration was necessary to exceed the fluorescence of the surface-bound avidin. The binding isotherm experiments were carried out for both B-DPPE and B-x-DPPE of various doping densities. The fluorescence intensities measured before PBS rinse were used for data analysis. A molecular weight of 67 000 Da for avidin was used in calculation.[18]

Analysis of Isotherm Data. In the avidin binding experiments, fluorescence intensity (F) was measured for a series of bulk avidin concentrations ([A]). The three parameters in eq 9, ω, K_0, and F_{max}, were determined by the least-squares fitting method.[17] An important step in the nonlinear regression algorithm was to calculate the residual, the difference between F obtained from experiment and that predicted by eq 9. Since eq 9 has no analytical solution for F, a numerical method was used to calculate F for given values of [A] and ω, K_0, and F_{max}.[17] All the computation was carried out on a DEC Workstation 2100.

Values for η were estimated from the fitted values of ω by assuming that the distribution of the receptors is a square lattice ($z = 4$); i.e. $\eta = \omega^{1/4}$. While other distributions were considered (e.g. hexagonal close packet), indirect support for our assumption comes from crystallographic data showing that streptavidin binds to biotinylated lipid monolayers at the air–water interface in a square lattice.[19]

ATR-FTIR of Surface-Bound Avidin. Attenuated total reflection (ATR) infrared spectra of avidin bound to biotin lipid doped LB films were collected on a Fourier transform infrared (FTIR) spectrometer (Bio-Rad FTS-60A, Cambridge, MA). ATR surface preparation exactly paralleled the EFO preparation procedure described elsewhere,[7,8] modified only by the differences in geometry of the two optical elements. Briefly, silicon ATR crystals (45° trapezoidal, 10 × 85 × 2 mm, 43 reflection, Harrick Scientific, Ossining, NY) were cleaned at room temperature in chromic acid and silanized with DDS. Monolayer films of AA doped from 0 to 5 mol % with either B-DPPE or B-x-DPPE with LB deposited onto both sides of the hydrophobic ATR crystals during the down stroke. ATR crystals deposited with biotin-lipid-doped monolayers were collected in a submerged polyethylene trough placed in the dipping well. The polyethylene trough was subsequently removed, while still filled with aqueous subphase, and placed in a larger vessel containing PBS buffer. The ATR crystals were assembled into a custom-built Lucite flow cell while still submerged, thus maintaining head-group-out orientation of the LB films. The flow cell assembly was mounted on the ATR accessory of the FTIR spectrometer and both sides of the ATR crystal were flushed with PBS buffer. The sample compartment was purged for 5 min, with dry CO_2-free air, and background adsorption spectra of the LB film and buffer were collected (1024 scans at 8 cm^{-1} resolution) and stored. A solution of 0.1 mg/mL avidin (Sigma) was introduced into the ATR/flow cell assembly and allowed to adsorb for 30 min followed by a 3× sample volume flush with PBS and a 5-min purge. Adsorbed protein spectra were collected using the same conditions as the background spectra and were background subtracted. ATR spectra of adsorbed native and denatured avidin also were collected as controls. Avidin was thermally denatured according to Kato et al.[11] By use of the same procedure as in the LB experiments, solutions of 0.1 mg/mL of either native or thermally denatured avidin were exposed to untreated silicon ATR crystals and allowed to adsorb. Peak locations and intensities were determined using manufacturer supplied software. Infrared band intensity ratios were calculated and plotted using Cricket Graph software.

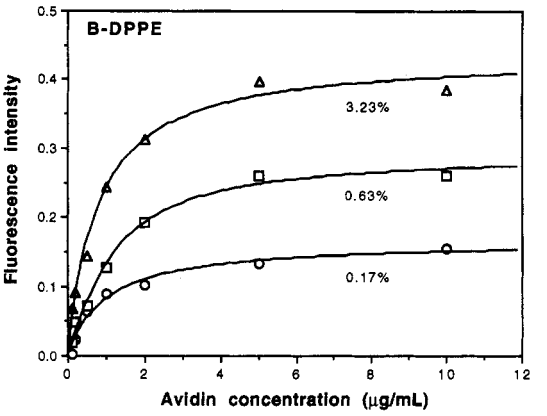

Figure 2. Isotherms of avidin binding to B-DPPE in LB monolayers. The three sets of data correspond to B-DPPE surface densities of 0.17 (open circles), 0.63 (filled circles), and 3.23 (triangles) mol %. The solid curves are the best fits of data to eq 9.

Results

EFO Study. Representative avidin binding isotherms obtained from experiments for various B-DPPE and B-x-DPPE doping densities are shown in Figures 2 and 3, respectively. The solid lines are the best fits of the data to eq 9. The three parameters, ω (or η^4), K_0, and F_{max}, were obtained from the data fitting and are listed in Table I (for B-DPPE) and Table II (for B-x-DPPE). Isotherms of avidin binding to B-DPPE (Figure 2) and low densities of B-x-DPPE (open symbols and dashed lines in Figure 3) had hyperbolic curves, suggesting no positive cooperativity. However, isotherms from surfaces with higher densities of B-x-DPPE had sigmoid curves (filled symbols and solid lines in Figure 3), suggesting fairly strong positive cooperativity. Tables II and III list the fitted parameters ω, K_0, and F_{max} in eq 9 for all of the binding isotherms performed with B-DPPE and B-x-DPPE doped LB films.

Figure 4 is a semilog plot of F_{max} vs the mol % of B-DPPE and B-x-DPPE in the LB film, where the nonspecific

(16) Haugland, R. P. *Handbook of Fluorescent Probes and Research Chemicals*; Molecular Probes, Inc.: Eugene, OR, 1989.
(17) Zhao, S. Experimental and modeling study of avidin binding to biotin in lipid monolayers. Ph.D. dissertation, Department of Biomedical Engineering, Duke University, 1992.
(18) Green, N. M. *Adv. Protein Chem.* **1975**, *29*, 85–133.
(19) Darst, S. A.; Ahlers, M.; Meller, P. H.; Kubalek, E. W.; Blankenburg, R.; Ribi, H. O.; Ringsdorf, H.; Kornberg, R. D. *Biophys. J.* **1991**, *59*, 387–396.

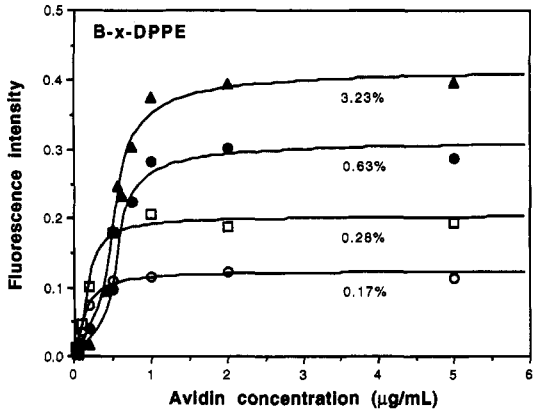

Figure 3. Isotherms of avidin binding to B-x-DPPE in LB monolayers. The four sets of data correspond to B-x-DPPE surface densities of 0.17 (open circles), 0.28 (squares), 0.63 (filled circles), and 3.23 (triangles) mol %. The solid curves are the best fits of data to eq 9.

Table I. Parameters ω, K_0, and E_{max} Determined from Isotherms of Avidin Binding to LB Monolayers Containing B-DPPE

biotin density (mol %)	ω	η	K_0 (10^7 M^{-1})	F_{max} (10^{-2})
0.0	1.78 ± 1.59	1.15 ± 0.26	19.2 ± 8.2	1.31 ± 0.07
0.17	0.983 ± 0.776	0.996 ± 0.197	6.61 ± 1.79	16.5 ± 1.3
0.28	13.4 ± 1.99	1.91 ± 0.07	2.48 ± 0.19	8.37 ± 0.12
0.40	0.459 ± 0.509	0.823 ± 0.23	17.3 ± 7.0	23.1 ± 2.2
0.50	0.10 ± 0.17	0.562 ± 0.24	58.1 ± 3.4	30.7 ± 3.8
0.63	2.06 ± 0.94	1.20 ± 0.14	3.95 ± 0.68	29.3 ± 1.4
0.76	4.14 ± 1.81	1.43 ± 0.16	3.30 ± 0.63	46.9 ± 2.0
0.99	7.74 ± 1.39	1.67 ± 0.07	2.87 ± 0.25	41.8 ± 0.7
1.41	3.91 ± 1.87	1.41 ± 0.17	4.01 ± 0.86	33.5 ± 1.4
2.70	0.448 ± 0.326	0.818 ± 0.149	11.3 ± 2.5	68.5 ± 5.2
3.23	1.13 ± 0.64	1.03 ± 0.15	7.82 ± 1.70	43.3 ± 2.3
4.76	4.93 ± 1.49	1.49 ± 0.11	5.06 ± 0.73	31.2 ± 0.8
16.7	0.774 ± 0.551	0.938 ± 0.17	6.70 ± 1.48	42.7 ± 3.4
100	2.60 ± 1.27	1.27 ± 0.16	4.09 ± 0.82	66.6 ± 3.2

Table II. Parameters ω, K_0, and F_{max} Determined from Isotherms of Avidin Binding to LB Monolayers Containing B-x-DPPE

biotin density (mol %)	ω	η	K_0 (10^7 M^{-1})	F_{max} (10^{-2})
0.17	4.61 ± 2.00	1.47 ± 0.16	20.3 ± 4.1	12.4 ± 0.4
0.28	12.0 ± 5.0	1.86 ± 0.19	9.88 ± 1.97	20.4 ± 0.5
0.40	4.78 ± 1.71	1.48 ± 0.13	7.01 ± 1.17	27.0 ± 0.9
0.50	7.88 ± 2.3	1.68 ± 0.12	5.67 ± 0.86	32.5 ± 0.9
0.63	28.9 ± 6.0	2.32 ± 0.12	2.14 ± 0.20	31.2 ± 0.9
0.76	21.3 ± 2.35	2.15 ± 0.06	2.04 ± 1.19	32.1 ± 0.4
0.99	54.8 ± 16.7	2.72 ± 0.21	1.46 ± 0.23	42.2 ± 1.3
1.41	53.3 ± 6.0	2.71 ± 0.08	1.49 ± 0.10	28.7 ± 0.4
1.79	36.4 ± 9.0	2.46 ± 0.15	2.28 ± 0.32	38.2 ± 1.3
2.17	19.0 ± 3.0	2.09 ± 0.08	2.70 ± 0.20	30.2 ± 0.7
3.23	22.1 ± 5.0	2.17 ± 0.12	2.66 ± 0.29	41.6 ± 1.4
6.25	23.6 ± 5.12	2.20 ± 0.12	2.04 ± 0.21	42.5 ± 1.5
16.7	46.0 ± 12.3	2.61 ± 0.17	1.60 ± 0.23	37.1 ± 1.7
100	32.3 ± 5.5	2.38 ± 0.10	2.43 ± 0.23	59.9 ± 1.4

binding of avidin to the LB monolayer was comparatively insignificant (Table I). As expected, F_{max} increased with the biotin lipid surface density but appears to level off at >1 mol % biotin lipid. Data in Figure 4 suggest that there is no significant difference between the amounts of avidin bound to monolayers with B-DPPE and B-x-DPPE at equilibrium.

Figure 5 is a semilog plot of the cooperativity coefficients (η) determined for avidin binding against the surface densities of B-DPPE and B-x-DPPE in the LB film. Note that η does not appear to change with B-DPPE surface density and had an average value of $\eta = 1.20 \pm 0.37$ (see

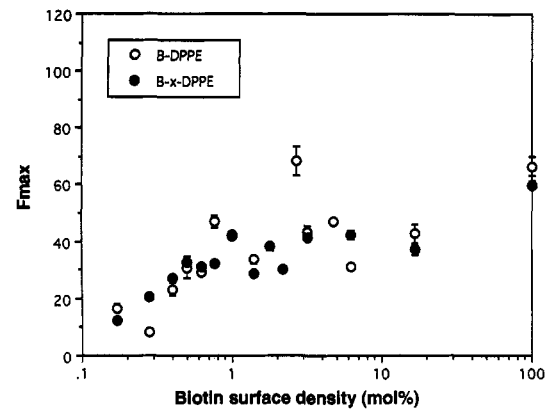

Figure 4. Maximum fluorescence intensities from avidin bound to B-DPPE (open circles) or B-x-DPPE (filled circles) of various surface densities.

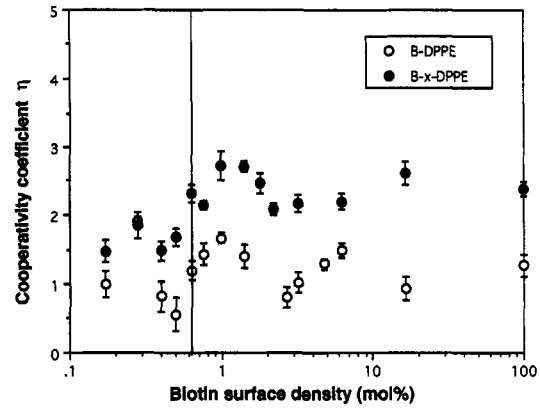

Figure 5. Cooperativity coefficients (η) of avidin binding to B-DPPE (open circles) or B-x-DPPE (filled circles) in LB monolayers. The vertical line indicates a biotin surface density of 0.63 mol %.

Table I). For B-x-DPPE, on the other hand, η increased with the B-x-DPPE density up to approximately 1 mol %, after which η appears to level off (see Table II). However, it is more interesting to correlate these results to the physical size of the avidin molecule, where 0.6 mol % is the approximate minimum receptor density necessary to bind a monolayer of avidin (see Discussion).

Statistical analysis at the 95% confidence level shows all η values for B-DPPE are not different from unity, and η values for ≥0.63 mol % B-x-DPPE are not different from their average value of $\eta = 2.38 \pm 0.24$. These results indicate that (1) avidin bound to B-DPPE receptors noncooperatively over the entire range of receptor densities, (2) avidin bound to B-x-DPPE exhibited positive cooperativity for receptor densities of ≥0.63 mol %, and (3) in both cases η was uncorrelated to mol % biotin lipid in the LB film for ≥0.63 mol %. The correlation of η to mol % biotin lipid for LB films of ≤0.63 mol % was determined by fitting these data to a straight line, yielding a slope of 1.45 ± 0.50 and intercept of 1.18 ± 0.19 (R^2 = 0.679) for B-x-DPPE (Student's t test: $p < 0.05$ for both slope and intercept), and a slope of −0.46 ± 1.96 and intercept of 1.26 ± 0.38 (R^2 = 0.050) for B-DPPE (Student's t test: $p > 0.5$ for slope, $p < 0.05$ for intercept). Thus, a fourth observation is that η increases with increasing receptor density for ≤0.63 mol % B-x-DPPE.

Of all binding experiments, five of them yielded η estimates of less than unity (Figure 5 and Table I), which is indicative of negative cooperativity. In four of these instances η is within a standard deviation (0.37) centered at 1.0 and, therefore, probably represents noncooperativity.

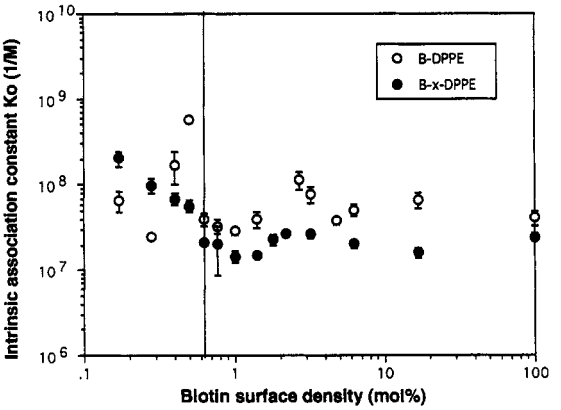

Figure 6. Intrinsic association constants (K_0) of avidin binding to B-DPPE (open circles) or B-x-DPPE (filled circles) in LB monolayers. The vertical line indicates a biotin surface density of 0.63 mol %.

Table III. Estimated Apparent Association Constant of Avidin Binding to LB Monolayers Containing B-DPPE or B-x-DPPE

biotin density (mol %)	K_{app} (10^7 M^{-1})	
	B-DPPE	B-x-DPPE
0.17	6.5	95
0.28	33	118
0.40	7.9	34
0.50	5.8	45
0.63	8.2	62
0.76	14	44
0.99	22	80
1.41	16	80
1.79	5.1	84
2.17	8.8	52
3.23	11	59
6.25	25	48
16.7	5.2	74
100	11	78
mean K_{app}	11 ± 8.1	68 ± 23

Only once was η significantly less than 1.0 (0.56 ± 0.24), suggesting a fairly strong negative cooperativity. It has been shown that Scatchard plots of binding isotherms can appear to be negatively cooperative if the "large-ligand effect" is present.[13-15,20] This effect can be observed when a large protein ligand binds noncooperativity to one or two receptors and at the same time inactivates (or covers) other neighboring receptors. Therefore, this effect is also called "pseudocooperativity". However, it is more plausible that this low cooperativity coefficient resulted from experimental error rather than an isolated occurrence of the large-ligand effect.

Figure 6 is a log-log plot of the intrinsic association constant K_0 against biotin surface density. K_0 values for the entire range of B-DPPE surface densities showed no correlation to the biotin receptor density in the LB monolayer and had an approximate average of (7 ± 5) × 10^7 M^{-1}. On the other hand, K_0 for B-x-DPPE dopant decreased quickly with increasing B-x-DPPE surface density and leveled off to an approximate average of (2.0 ± 0.6) × 10^7 M^{-1} for B-x-DPPE densities of ≥0.63 mol % (the vertical dashed line).

The apparent association constant (K_{app}) is the association constant observed at equilibrium. If virtually all accessible biotin groups are bound at equilibrium, then K_{app} can be approximated from eq 5, i.e. $K_{app} \approx K_0\eta^4$. Table III contains the estimated values of K_{app} for B-DPPE and B-x-DPPE. The average values of K_{app} for B-DPPE and B-x-DPPE are (11 ± 8) × 10^7 M^{-1} and (68 ± 23) × 10^7 M^{-1}, respectively. K_{app} appears to be independent of receptor doping density, but the average value of K_{app} for B-x-DPPE receptor is approximately 6 times greater than that for B-DPPE.

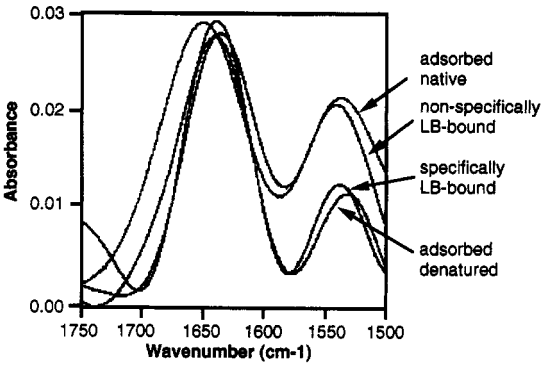

Figure 7. Amide I and II bands of background-subtracted ATR-FTIR spectra of native avidin and thermally denatured avidin adsorbed to bare silicon ATR crystals, nonspecifically LB-bound avidin (AA film with 0 mol % biotin lipid), and specifically LB-bound avidin (AA with 0.5 mol % B-DPPE).

ATR-FTIR Study. Figure 7 compares background-subtracted, unmassaged, ATR-FTIR spectra of (1) native avidin and (2) thermally denatured avidin adsorbed to bare silicon ATR crystals, (3) avidin nonspecifically adsorbed to an AA film without biotin lipid, and (4) avidin specifically bound to a biotin-lipid-doped AA film (0.5 mol % B-DPPE). The amide I and amide II bands of avidin are evident in Figure 7 at 1640 and 1540 cm^{-1}, respectively. It is apparent from Figure 7 that the ATR spectrum of specifically LB-bound avidin differs significantly from the spectra of adsorbed native avidin and nonspecifically LB-bound avidin and more closely resembles the spectrum of adsorbed denatured avidin.

Table IV lists the wavenumber locations of the amide I and amide II band maxima, and the ratio of the amide II to amide I band intensities, for avidin bound to LB films doped from 0 to 5 mol % biotin lipid and for native and thermally denatured avidin adsorbed to bare ATR crystals. The amide I and II band maxima, respectively, appeared as follows: 1536 and 1648 cm^{-1} for adsorbed native avidin; 1531 and 1635 cm^{-1} for adsorbed denatured avidin; and 1538–1542 cm^{-1} and 1638–1637 cm^{-1} for both nonspefically and specifically LB-bound avidin. Therefore, the amide I and II band maxima of denatured avidin were shifted to lower wavenumbers than that observed for all of the LB-bound avidin spectra, while only the amide II maxima of native avidin was shifted significantly from that observed with LB-bound avidin.

The intensity of the amide I band for LB-bound avidin increased and then leveled off with increasing mol % biotin lipid, whereas the amide II band intensity initially decreased with increasing mol % biotin lipid and then appeared to vanish from the ATR spectrum before returning at higher doping densities. When viewed as the ratio of the amide II and amide I band intensities (Table IV), the ATR data seem to represent a loss of and then an apparent return to a native conformation, where the maximum conformational change occurred at 0.25, 0.50,- and 0.75 mol % for B-x-DPPE and at 0.75, 1.0, and 2.5 mol % for B-DPPE. However, it seems unlikely that surface bound avidin would become more conformationally altered than thermally denatured avidin, and the curious disappearance of the amide II band may be an artifact of the background subtraction process. For example, biotin has a strong absorption at 1550 cm^{-1} [10] that may have

(20) McGhee, J. D.; von Hippel, P. H. *J. Mol. Biol.* 1974, *86*, 469–489.

Table IV. Amide I and Amide II Band Locations and Ratio of Band Intensities of Adsorbed and LB-Bound Avidin

surface of ATR crystal	amide II/amide I band locations (cm^{-1})		amide II/amide I intensity ratio	
bare surface, native avidin	1648/1536		0.72	
bare surface, denatured avidin	1635/1531		0.15	
biotin-free LB film, native avidin	1638/1542		0.78	
biotin-containing LB films, native avidin				
mol % biotin lipid	B-DPPE	B-x-DPPE	B-DPPE	B-x-DPPE
0.10	1638/1542	1638/1538	0.49	0.19
0.25	1638/1541	*a*/1538	0.35	*a*
0.50	1637/1539	*a*/1539	0.15	*a*
0.75	*a*/1537	*a*/1538	*a*	*a*
1.00	*a*/1536	1637/1540	*a*	0.09
2.50	*a*/1538	1638/1540	*a*	0.57
5.00	1638/1538	1638/1540	0.08	0.83

[a] Discernible absorption peak not identified.

obscured a weak avidin amide II band when background subtracted, while the spectrum of adsorbed denatured avidin was collected on a bare ATR crystal. Nonetheless, one can conclude from the ATR measurements that biotin lipid bound avidin becomes conformationally altered, and the greater extent of conformational change occurs at a lower receptor density for B-x-DPPE than for B-DPPE.

Discussion

Positive cooperativity refers to activity that facilitates ligand binding by the presence of other ligand participants, while negative cooperativity concerns activity that hinders ligand binding. Noncooperativity corresponds to the binding where all participants act independently. Theories have been developed that ascribe cooperativity to intra-protein and interprotein interactions that require the participating moieties to be in proper juxtaposition.[21-23] Conformational changes of the protein or its subunits are considered to be essential in inducing cooperativity in these theories. Chay and Cho[24] proposed that cooperativity can also arise in biological membranes as a consequence of microenvironmental change. Specifically, if a ligand has preferential binding to either a protonated or an unprotonated state of the protein and if the net charge of the liganded state is different from unliganded state, the existence of two environments may induce cooperativity.

Streptavidin is a protein of bacterial origin that shares the same high binding affinity for biotin as egg white avidin.[6] Blankenburg et al.[25] observed apparent protein–protein interaction in their study of streptavidin binding to biotinylated phospholipid monolayers at the air–water interface. Streptavidin was observed to form highly ordered domains at the air–water interface, but only when biotin lipid receptors were present in the monolayer, suggesting that binding with biotin was necessary for the streptavidin–streptavidin interaction to occur. Interestingly, they demonstrated that the presence of a highly organized monolayer, i.e. the solid-condensed state, is not necessary for the formation streptavidin domains. These domains were observed even when the biotin lipid monolayer was in the uncompressed state. This observation indicates that streptavidin is driven to aggregation, i.e. "swim around", after they bind with biotin. Blankenburg et al. also showed that the lack of a spacer between the hydrophobic tails and the biotin head group in the lipid prevents streptavidin binding to biotin. However, when they substituted avidin for streptavidin, no protein domains were observed through light microscopy. Ku et al. recently used electron microscopy to show that avidin also forms domains on biotin lipid monolayers at the air–water interface, albeit very small ones.[26] The difference in domain size suggests that the interaction between biotin-bound avidin molecules is more combersome than that between the biotin-bound streptavidin.

In the current paper, our estimates of the cooperativity coefficient (Tables I and II, Figure 5) indicate that two conditions were necessary for the occurrence of positive cooperativity: (1) a sufficiently high biotin surface density; (2) good access of the biotin group in the LB film to the binding avidin molecules.

Clearly, if individual receptors are too far apart, protein–protein interactions do not occur. This point is supported by considering a receptor density of 0.63 mol % biotin lipid in the LB monolayer; which is close to the approximate minimum receptor density of 0.6 mol % necessary to bind a contiguous monolayer of avidin. [(3025–47)/18 $\approx$ 165 AA molecules per single biotin lipid per 3025 Å^2, where 3025 Å^2 (55 Å × 55 Å),[18] 47 Å^2, and 18 Å^2 are the molecular areas of biotin lipid–bound avidin, a biotin lipid, and an AA fatty acid, respectively.[17] (1/165) × 100 = 0.6 mol % biotin lipid in the LB film therefore corresponds to the minimum receptor density needed to bind a contiguous monolayer of avidin.] Thus, it is not surprising that noticeably sigmoid binding curves were observed only for experiments with ≥0.63 mol % B-x-DPPE (Figure 3 and Table II) where the avidin molecules are sufficiently close to interact. However, η appears to increase up to 1 mol % B-x-DPPE (Figure 5), suggesting that the level of cooperativity continues to increase until most of the avidin molecules are bound by two B-x-DPPE receptors (e.g. >1.2 mol %).

The explanation for the second condition is somewhat more speculative and may be related to the conformation of the surface-bound avidin. That is, since cooperativity was observed only with the more accessible B-x-DPPE biotin lipid, we hypothesize that avidin bound to B-x-DPPE was conformationally altered in a manner that contributed to the cooperativity observed in our study. Indirect support for this hypothesis can be inferred again from streptavidin.

Streptavidin, like avidin, consists of four identical subunits, each with a single high affinity biotin binding

(21) Monod, J.; Wyman, J.; Changeux, J.-P. *J. Mol. Biol.* **1965**, *12*, 88–118.
(22) Koshland, D. E.; Nemethy, G.; Filmer, D. *Biochemistry* **1966**, *5*, 365–385.
(23) Changeux, J.-P.; Thiery, J.; Tung, Y.; Kittel, C. *Proc. Natl. Acad. Sci. U.S.A.* **1967**, *57*, 335–341.
(24) Chay, T. R.; Cho, S.-H. *Biophys. Chem.* **1982**, *15*, 271–275.
(25) Blankenburg, R.; Meller, P.; Ringsdorf, H.; Salesse, C. *Biochemistry* **1989**, *28*, 8214–8221.
(26) Ku, A. C.; Darst, S. A.; Kornberg, R. D.; Robertson, C. R.; Gast, A. P. *Langmuir* **1992**, *8*, 2357–2360.

site. Weber et al.[27] used X-ray crystallography to show that the biotin binding pockets of streptavidin lie at the end of β barrels, and biotin binding involves "displacement of bound water, formation of multiple interactions between biotin heteroatoms and the binding site residues, and the burial of biotin through ordering of a surface loop. Since streptavidin shares many similarities with avidin, including 38% sequence homology,[6] it is reasonable that biotin-bound avidin undergoes a similar a conformational change and that this change is greatest when the biotin head group is accommodated deeply in the binding pocket. Unfortunately, analogous crystallographic data are not yet available for avidin, and one is tempted to use what is known definitively about streptavidin to infer information about avidin. However, such extrapolations should be made with caution.

Raman and Fourier transform infrared (FTIR) are complementary spectroscopy techniques commonly used to determine the secondary structure of macromolecules.[28,29] The main vibrational absorptions of proteins are the N—H stretch ($\sim$3300 cm^{-1}), amide I (C=O stretch, $\sim$1640 cm^{-1}), amide II (N—H bend, C—N stretch, $\sim$1550 cm^{-1}) and amide III (mixed N—H and C—N vibrations, $\sim$1250 cm^{-1}) absorptions. Honzatko and Williams[30] used Raman spectroscopy to determine that avidin consisted of 55% β-sheet and 10% α-helix conformation, but observed virtually no difference in the amide I and amide II regions in solution phase Raman spectra of avidin and the avidin biotin complex. Barbucci et al.[10] used ATR-FTIR to examine the amide bands of avidin and the avidin–biotin complex, assigning α structure to absorptions at 1668, 1307, and 1275 cm^{-1} and β structure to absorptions at 1630 and 1250 cm^{-1}, but did not assign structure to the 1540-cm^{-1} amide II absorption band. Barbucci et al. also observed only minor differences in the ATR-FTIR spectrum of the avidin–biotin complex when compared to a summed spectrum of avidin and biotin. Note that both Honzatko and Williams and Barbucci et al. collected spectra from extremely concentrated (i.e. 100 mg/mL) avidin solutions.

In order to investigate the possibility of a conformational change in surface-bound avidin, we performed a series of ATR-FTIR measurements including native and denatured avidin adsorbed to bare ATR crystals, avidin nonspecifically bound to biotin-free LB films, and avidin specifically bound to biotin-lipid-doped LB films. Contrary to the solution phase work of Honzatko and Williams[30] and Barbucci et al.,[10] we observed significant spectral differences between the adsorbed, nonspecifically LB-bound, and specifically LB-bound cases (Figure 8). However, unlike the above reports, there were no bulk contributions to any of our spectra, and all of our data were derived strictly from monolayer and submonolayer films of avidin. Using the intensity ratio technique of Kato et al.,[11] it also appears that specifically LB-bound avidin experienced conformational changes that were effected by both the biotin lipid surface density and the biotin lipid accessibility (Table IV). Unfortunately, signal averaging 1024 scans at 8 cm^{-1} resolution smoothed out the fine structure in the data, making it difficult to resolve the primary amide I and amide II absorbances into the subpeaks and shoulders observed by Barbucci et al.[10] The lower absorbances also led to difficulty in discerning the amide II peak when it fell into noise (see Results). Therefore, our ATR results are by no means definitive but do provide evidence that a conformational change occurs when avidin binds a biotin lipid at a surface and that the conformational change is qualitatively different for avidin bound to B-x-DPPE than to B-DPPE.

Finally, the intrinsic association constant K_0 determined for LB films doped with B-DPPE did not show a clear trend (Figure 6), suggesting that B-DPPE surface density did not significantly affect the affinity of avidin for the biotin group in the LB film. However, K_0 decreased linearly with increasing B-x-DPPE surface density until approximately 0.63 mol %, after which is leveled off. In a previously published, independent experiment we similarly observed that the kinetic rate of avidin binding to B-x-DPPE doped LB films decreased rapidly with increased receptor density and then leveled off at a steady value.[8] In that study it was reasoned that a drop in binding affinity resulted from a decreased accessibility of avidin to the individual B-x-DPPE receptors as the receptor density increased. When doping density was 0.63 mol % or higher, it is not clear why K_0 values for B-x-DPPE ($K_{0,ave}$ = (2.0 ± 0.6) × 10^7 M^{-1}) were on the average slightly smaller than those for B-DPPE ($K_{0,ave}$ = (7 ± 5) × 10^7 M^{-1}). A possible explanation might be that greater steric hindrance arose from neighboring B-x-DPPE than from neighboring B-DPPE.[8] However, the estimated apparent association constant K_{app} for B-x-DPPE was approximately 6 times greater than the corresponding K_{app} for B-DPPE (Table III).

Summary

An expression for the isotherm of cooperative protein binding to an array of receptors was developed and tested experimentally using the avidin–biotin lipid ligand–receptor system. Quantitative information on the intrinsic affinity of avidin for biotin in LB monolayers and the level of cooperativity was obtained by fitting experimental data to this model through nonlinear regression. Cooperative binding was observed only for the more accessible B-x-DPPE ligand and only at receptor densities of ≥0.63 mol %, which is sufficient to bind a near monolayer of avidin. From these results we conclude that the avidin–avidin interactions necessary for cooperative binding occurred when two conditions were met: (1) biotin surface density was high enough to provide adequate proximity of binding sites; (2) the biotin groups were extended sufficiently above the LB monolayer so they would fit with facility into the binding pocket of avidin. Based upon available data for streptavidin, we postulate that facile binding of the B-x-DPPE ligand by avidin resulted in a conformation change on the protein that promoted cooperative activity. ATR-FTIR studies provided evidence that a conformational change occurred in avidin when it bound biotin lipid in the LB film and that this conformational change was at least qualitatively different for avidin bound to B-DPPE and to B-x-DPPE.

Acknowledgment. This work was funded by a biomedical research grant from the Whitaker Foundation, NIH Grant HL 32132, and a graduate fellowship from the NSF/ERC Center for Emerging Cardiovascular Technologies at Duke University. We thank Dr. G. A. Truskey of Duke University for his keen advice and helpful discussion. An anonymous reviewer is thanked for providing the analysis presented in Appendix B.

(27) Weber, P. C.; Ohlendorf, D. H.; Wendoloski, J. J.; Salemme, F. R. *Science* **1989**, *243*, 85–88.
(28) Colthup, N. B. *Introduction to Infrared and Raman Spectroscopy*, 3rd ed.; Academic Press: Boston, MA, 1990.
(29) Parker, F. S. *Applications of Infrared Spectroscopy in Biochemistry, Biology, and Medicine*; Plenum Press: New York, 1971.
(30) Honzatko, R. B.; Williams, R. W. *Biochemistry* **1982**, *21*, 6201–6205.

Appendix A: Association Constant as a Function of Free Energy Change

The binding of a protein ligand (A) to its receptor (B) on a surface can be treated as a bimolecular reaction

$$A + B \rightleftharpoons AB \tag{A1}$$

The equilibrium constant K_e for this reaction is defined as $K_e = a_{AB}/(a_A a_B)$, where a_A, aB, and a_{AB} are the activities of species A, B, and AB at equilibrium, respectively.[31] In a dilute solution of nonelectrolytes the activity of a species is equal to its mole fraction in the solution.[31] Thus the equilibrium constant can be expressed as

$$K_e = \frac{X_{AB}}{X_A X_B} \tag{A2}$$

where X_A, X_B, and X_{AB} are the mole fractions of species A, B, and AB at equilibrium, respectively. Since mole fraction of a species is proportional to its concentration, X_A, X_B, and X_{AB} can be written as $X_A = \alpha_A[A]$, $X_B = \alpha_B[B]$, and $X_{AB} = \alpha_{AB}[AB]$, where [A], [B], and [AB] are the concentrations of species A, B, and AB at equilibrium, respectively, and α_A, α_B, and α_{AB} are proportionality constants which convert the units of concentration to mole fractions. Because the units for [B] and [AB] are the same (e.g., moles per unit area), α_B equals α_{AB}, yielding

$$K_e = K/K_\alpha \tag{A3}$$

where

$$K = \frac{[AB]}{[A][B]} \qquad K_\alpha = \frac{\alpha_A \alpha_B}{\alpha_{AB}} = \alpha_A \tag{A4}$$

For any chemical reaction, the equilibrium association constant K_e is related to the standard free energy change ΔG by $\Delta G = -RT \ln K_e$, where R is the universal gas constant and T is temperature in Kelvin.[31] Using this relation and eq A3, we obtain the expression of K as a function of ΔG

$$K = K_\alpha \exp(-\Delta G/RT) \tag{A5}$$

Appendix B: Average Number of Protein-Bound Neighboring Receptors

To model protein binding to the biotin-lipid receptors, it is necessary to determine the statistical average of the number of protein-bound nearest neighboring receptors (n). This in turn requires assuming a receptor distribution. The simplest receptor distribution is a square lattice represented by the matrix (Figure 8)

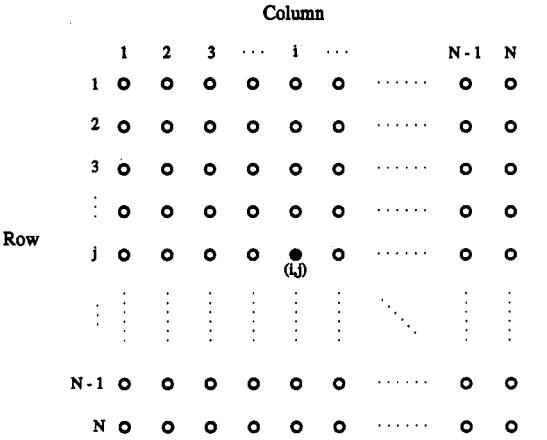

Figure 8. Matrix representation of an ideal square lattice of protein receptors. Each open circle represents a receptor. Each receptor has four nearest neighbors.

$$S_{i,j} = \begin{cases} S_{i,j} = 1 \text{ if receptor } i,j \text{ is occupied} \\ S_{i,j} = 0 \text{ if receptor } i,j \text{ is vacant} \end{cases} \tag{B1}$$

The number of occupied sites neighboring a given receptor $s_{i,j}$ is given by $s_{i-1,j} + s_{i+1,j} + s_{i,j+1} + s_{i,j-1}$. Therefore, the average number of nearest neighboring receptors occupied by protein (n) is given by

$$n = \frac{1}{N} \sum_{i=1}^{N} \sum_{j=1}^{N} (s_{i-1,j} + s_{i+1,j} + s_{i,j+1} + s_{i,j-1}) \tag{B2}$$

where N is the total number of receptors. Assuming array is infinite (N is very large), the four terms in eq B2 are equivalent and eq B2 becomes

$$n = \frac{4 \sum_{i=1}^{N} \sum_{j=1}^{N} s_{i,j}}{N} \tag{B3}$$

The dual summation in the numerator in eq B3 is simply the number of protein-bound receptors, which divided by the total receptors N, is the fraction of bound receptors x_1. Therefore, eq B3 becomes

$$n = 4x_1 \tag{B4}$$

(31) Klotz, I. M.; Rosenberg, R. M. *Chemical Thermodynamics*, 4th ed.; Benjamin/Cummings, Menlo Park, CA, 1986; pp 354.